Eur. Phys. J. AP **21**, 151–159 (2003)
DOI: 10.1051/epjap:2002122

THE EUROPEAN PHYSICAL JOURNAL APPLIED PHYSICS

Causal modeling and identification of a travelling wave ultrasonic motor

F. Giraud[a] and B. Lemaire-Semail

Laboratoire d'Électrotechnique et d'Électronique de Puissance de Lille, EUDIL-USTL, avenue Paul Langevin, 59655 Villeneuve d'Ascq Cedex, France

Received: 2 April 2002 / Received in final form: 10 September 2002 / Accepted: 22 October 2002
Published online: 19 December 2002 –

Abstract. This paper deals with the causal modeling of a Traveling Wave Ultrasonic Motor; the aim of the study is to build an approach which may take into account the physical contact responsible for the pull-out phenomenon, but straightforward enough to be useful for control. As the parameters available for the modeling can not be obtained following the well known electromechanical equivalent scheme identification, a new identification method is proposed. In this purpose, the model of the motor is expressed in the traveling wave rotating frame.

PACS. 77.65.-j Piezoelectricity and electromechanical effects – 84.50.+d Electric motors – 43.38.Fx Piezoelectric and ferroelectric transducers

1 Introduction

Traveling Wave Ultrasonic Motors (TWUM) use the propagation of a bending wave at the thin plate surface to let a rigid ring revolve. This proceeding endows these motors high torque–low speed characteristics, and they become very interesting for applications in the field of positioning; one of the most well known industrial applications is the Canon's USM lense which uses these motors in the auto-focus system [1].

Unfortunately, TWUM are very sensitive to the external operating conditions, such as temperature, and it becomes hard to drive them. The modelization is then critical because it is the basis of the control scheme.

Some modeling of those motors finely describe the contact mechanism [2]. The good accuracy of the results is obtained at the expense of a complex modeling, very delicate to use for a control scheme. Some others use the electric equivalent circuit, useful for the steady state, but transitory operations are not validated.

So, this article proposes a new modelization, based on an energy study of the system. The contact mechanism effects are globalized in order to make the modeling simple enough to be used in the control. Once the proposed modeling structure is validated, the TWUM is described in a rotating reference frame in order to identify the significant parameters from experimental trials.

[a] e-mail: frederic.giraud@eudil.fr

2 Causal modeling in the stationary waves' fixed frame

2.1 Description of the studied piezoelectric motor

A description of those motors is given by [3]. Piezoelectric elements are bonded on a metal ring shaped **stator**. They are grouped together in two phases, named α and β respectively fed by the voltages v_α and v_β, the RMS value of which are V_α and V_β. The poling direction of these elements let an elastic flexural wave travel. This wave is assumed to be purely sinusoidal (hypothesis H_1). Moreover, we count k piezoelectric elements per phase with the same poling direction.

The traveling wave bending the ring uses friction to transmit torque to the **rotor shaft**, a metal component placed on the stator. The mass of the rotor shaft is called m_R. Figure 1 shows an illustration of the major components of the motor and several notations used along this article:

- a and b the respectively inner and outer radius of the stator;
- h the length between the undeformed centerline of the stator, and the position of the contact point;
- F_τ an axial force pressing the stator and the rotor together.

The rotor drives a load, and the inertia of the load and the rotor is named J. A load torque C_r acts on the mechanical system.

In order to make the modelization easier, and thus well adapted for a control scheme, we introduce the concept of

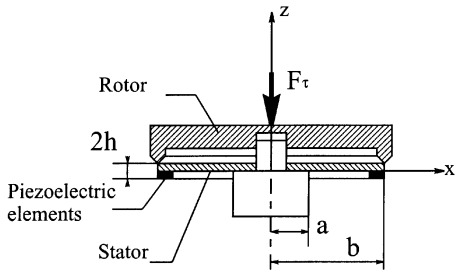

Fig. 1. Drawing of the studied motor.

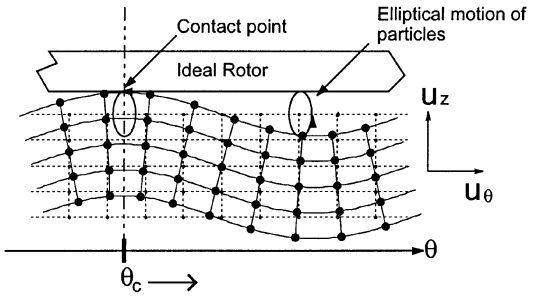

Fig. 2. Flexural wave in a plate.

ideal rotor. This element has a punctual (H_2) and a non-sliding contact (H_3) with the stator. Of course, friction will be considered between this ideal rotor and the real one. Finally, the materials are supposed to be linear (H_4).

Two **coordinates systems** are defined to locate each point of the stator before and after deformation. $\Re_1$, for which polar coordinates (r, θ, z) are used, is fixed, whilst $\Re_\theta$ is a rotating frame, and uses Cartesians coordinates [4].

2.2 Bending wave in the stator

When the piezoelectric elements of the phases α and β are fed , they create flexural strains which bend the stator. Each point $M(r, \theta, z)_{/\Re_1}$ of the stator moves to M' and the vector

$$\overrightarrow{MM'} = (u(r, \theta, z, t), v(r, \theta, z, t), w(r, \theta, z, t))$$

relatively $\Re_\theta$, is called displacement vector. Under assumption H_1, it is possible to give an expression of the displacement along axis z and for $r = b$ [3]:

$$w = w_\alpha(t)\cos(k\theta) + w_\beta(t)\sin(k\theta). \quad (1)$$

Two time varying functions, w_α and w_β, appear in this equation. In fact, when α is powered alone, a stationary wave is generated with an amplitude called w_α, and an other stationary wave exists when β is fed alone. And if both of the two phases are powered, the resulting wave is the sum of these two stationary waves according to H_4; w_α and w_β are also called the modal amplitudes, and their variations will be calculated in Section 2.3.

If the stator is supposed to be very thin so as to be considered as a plate, the Kirchoff assumption is valid, and the displacement along u_θ is then a function of w: $v = -\frac{z}{r}\frac{\partial w}{\partial \theta}$.

$$v(b, \theta, h) = -k\frac{h}{b}\left(-w_\alpha(t)\sin(k\theta) + w_\beta(t)\cos(k\theta)\right). \quad (2)$$

The wave's crest is located at the point for which displacement along z is maximum. If we call θ_c this position,we have:

$$\left.\frac{\mathrm{d}w}{\mathrm{d}\theta}\right|_{\theta=\theta_c} = 0. \quad (3)$$

And according to relation (1):

$$\theta_c = \frac{1}{k}\arctan\frac{w_\beta(t)}{w_\alpha(t)}. \quad (4)$$

We also define the height of the wave at the crest $\hat{W}$ by

$$\begin{aligned}\hat{W}(t) &= w(r = b, \theta = \theta_c, z = h)\\ &= w_\alpha(t)\cos(k\theta_c) + w_\beta(t)\sin(k\theta_c)\\ &= \sqrt{w_\alpha(t)^2 + w_\beta(t)^2}. \end{aligned} \quad (5)$$

We can now write down two other expressions for w and v:

$$\begin{aligned} w &= \hat{W}\cos(k\theta_c - k\theta)\\ v &= -k\frac{h}{b}\hat{W}\sin(k\theta_c - k\theta). \end{aligned} \quad (6)$$

The stator is a mechanical resonator, so the modal amplitudes w_α and w_β are sinusoidal functions of time. An elliptical rolling motion, as described by equation (6) is observed at the stator's surface; this motion is able to drive an ideal rotor pressed on the stator. The position where the stator makes contact with the ideal rotor is named contact point and is located at $\theta = \theta_c$. The flexural wave is depicted Figure 2.

Motion in the normal direction, and motion about the normal direction are the two degrees of freedom the motor have. We call V_{Nid} and V_{Tid} the velocities of the ideal *rotor* at $\theta = \theta_c$. Thanks to assumption H_2 and H_3, this velocity is equal to the *stator*'s wave velocity at the contact point, so as to we can write:

$$\begin{aligned} V_{Nid} &= \left.\frac{\mathrm{d}w}{\mathrm{d}t}\right|_{\theta=\theta_c} = \dot{w}_\alpha\cos(k\theta_c) + \dot{w}_\beta\sin(k\theta_c)\\ V_{Tid} &= \left.\frac{\mathrm{d}v}{\mathrm{d}t}\right|_{\theta=\theta_c} = -k\frac{h}{b}\left(-\dot{w}_\alpha\sin(k\theta_c) + \dot{w}_\beta\cos(k\theta_c)\right). \end{aligned} \quad (7)$$

Let $V_{Tid} = -k\frac{h}{b}V'_{Tid}$. In the purpose of simplification of equation (7), we can introduce the well known rotation matrix of angle $k\theta_c$,

$$R(k\theta_c) = \begin{pmatrix}\cos(k\theta_c) & -\sin(k\theta_c)\\ \sin(k\theta_c) & \cos(k\theta_c)\end{pmatrix} \quad (8)$$

to finally write down:

$$\begin{pmatrix} V_{Nid} \\ V'_{Tid} \end{pmatrix} = R(-k\theta_c) \begin{pmatrix} \dot{w}_\alpha \\ \dot{w}_\beta \end{pmatrix}. \quad (9)$$

The rotational speed of the ideal rotor, is given by: $\Omega_{id} = \frac{1}{b} V_{Tid}$.

Thus, it has been shown that a relationship exists between the amplitude of the two stationary waves generated by the piezoelectric elements and the kinetic of a rotor in contact with the stator. But we must now find the equations which depict the evolution of those waves as a function of the external forces, and the voltages v_α and v_β.

2.3 Stator's vibration equation

The ring shaped stator is a mechanical vibrator, forced by the voltages v_α and v_β. The vibration equation can be obtained from the derivation of the global energy of this system, in accordance with Hamilton's principle [5,6]. The modal amplitudes w_α and w_β are the key parameters to calculate this energy, which is made of kinetic, potential and electric energies. The final equation is given by:

$$\begin{pmatrix} m & 0 \\ 0 & m \end{pmatrix} \begin{pmatrix} \ddot{w}_\alpha \\ \ddot{w}_\beta \end{pmatrix} + \begin{pmatrix} d_s & 0 \\ 0 & d_s \end{pmatrix} \begin{pmatrix} \dot{w}_\alpha \\ \dot{w}_\beta \end{pmatrix} + \begin{pmatrix} c & 0 \\ 0 & c \end{pmatrix} \begin{pmatrix} w_\alpha \\ w_\beta \end{pmatrix} = \begin{pmatrix} AC_c & 0 \\ 0 & AC_c \end{pmatrix} \begin{pmatrix} v_\alpha \\ v_\beta \end{pmatrix} - \begin{pmatrix} f_{r\alpha} \\ f_{r\beta} \end{pmatrix}. \quad (10)$$

The electrical reaction is given by the motional current

$$\begin{pmatrix} i_{m\alpha} \\ i_{m\beta} \end{pmatrix} = AC_c \begin{pmatrix} \dot{w}_\alpha \\ \dot{w}_\beta \end{pmatrix}. \quad (11)$$

The parameters are:

- m: model mass of stator and ceramic
- c: stator's equivalent stiffness
- d_s: structural damping
- AC_c: elongation factor
- $(f_{r\alpha}, f_{r\beta})^t$: modal forcing vector.

The modal forces have been added in order to take into account the effect of external forces F_N and F_T that act on the wave:

- F_N in the axial direction; due to F_τ plus the dynamic effect of the rotor;
- F_T in the tangential direction; due to the torque.

These modal forces are calculated in the next section.

2.4 Calculation of the modal forcing vector

When a precise modelization of the contact mechanism is done to describe the rotor-stator interface, for example using friction Coulomb's laws, the modal forcing vectors are non linear, and the calculation is quite difficult to achieve [2,6].

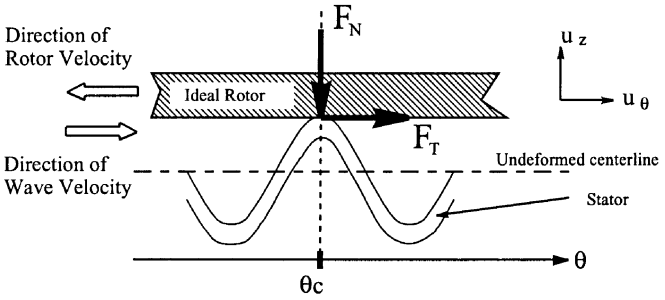

Fig. 3. Stator deformation and orientations of the external forces at the contact point.

But introducing the ideal rotor, and the assumption of a punctual contact, the calculation of the effect of the external forces F_N and F_T on the wave becomes much easier, as it can be seen along this section.

Figure 3 depicts the forces which act on the stator and their orientation, in the $\Re_\theta$ reference frame.

According to the Hamilton's principle, the variational power δp due to the forces F_N and F_T at the stator-rotor interface must be equal to the one dissipated by the modal forces. So, we write [7]:

$$\delta p = -f_{r\alpha}\delta\dot{w}_\alpha - f_{r\beta}\delta\dot{w}_\beta. \quad (12)$$

By definition, the power dissipated by the external forces at the stator-rotor interface, is simply expressed when the contact is punctual (see Fig. 3 for orientations):

$$\begin{aligned} \delta p &= F_T\delta V_{Tid} - F_N\delta V_{Nid} \\ &= -k\frac{h}{b}F_T\left(-\delta\dot{w}_\alpha(t)\sin(k\theta_c) + \delta\dot{w}_\beta(t)\cos(k\theta_c)\right) \\ &\quad - F_N(\delta\dot{w}_\alpha(t)\cos(k\theta_c) + \delta\dot{w}_\beta(t)\sin(k\theta_c)) \\ &= -\left(\cos(k\theta_c))F_N - k\frac{h}{b}\sin(k\theta_c)F_T\right)\delta\dot{w}_\alpha \\ &\quad - \left(\sin(k\theta_c)F_N + k\frac{h}{b}\cos(k\theta_c)F_T\right)\delta\dot{w}_\beta. \end{aligned} \quad (13)$$

Let $F'_T = k\frac{h}{b}F_T$. When identifying (12) and (13), the expression for $f_{r\alpha}$ and $f_{r\beta}$ appears:

$$\begin{pmatrix} f_{r\alpha} \\ f_{r\beta} \end{pmatrix} = \begin{pmatrix} \cos(k\theta_c)F_N - \sin(k\theta_c)F'_T \\ \sin(k\theta_c)F_N + \cos(k\theta_c)F'_T \end{pmatrix}. \quad (14)$$

Once again, it is possible to introduce $R(k\theta_c)$, and a simplification occurs:

$$\begin{pmatrix} f_{r\alpha} \\ f_{r\beta} \end{pmatrix} = R(k\theta_c) \begin{pmatrix} F_N \\ F'_T \end{pmatrix}. \quad (15)$$

2.5 Modelization of the real rotor

The kinematic of the ideal rotor is given by the instantaneous stator's velocity at the wave's crest. It is sufficient for this element because its mass is supposed to be null.

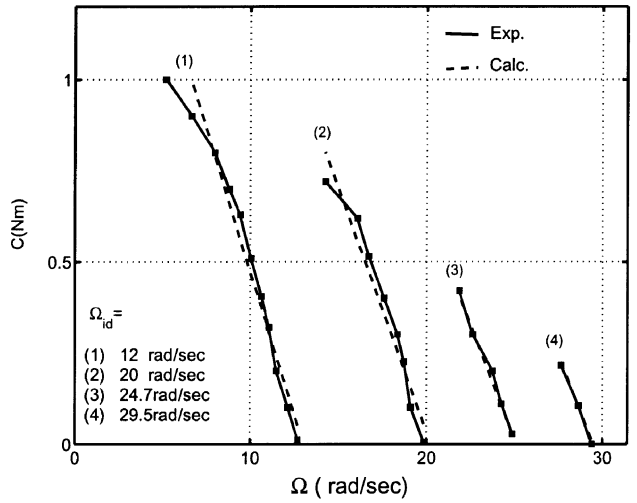

Fig. 4. Measured torque as a function of the rotational speed, for several values of Ω_{id}.

But we must now find out the dynamic equation of the real rotor which drives the load.

Let Ω and V_N respectively the rotational and the normal speed of the real rotor. The dynamic equation along axis z lets us write the vertical motion equation:

$$m_R \frac{\mathrm{d}V_N}{\mathrm{d}t} = F_N - F_\tau. \tag{16}$$

The same process leads to the equation of rotational motion:

$$J \frac{\mathrm{d}\Omega}{\mathrm{d}t} = C - C_r. \tag{17}$$

Moreover, we must express the coupling mechanisms between the two rotors (ideal and real). Because friction appears at the contact interface we can suggest for the rotational axis:

$$C = f(\Omega_{id} - \Omega). \tag{18}$$

An experimental justification of relation (18) can be found at Figure 4 which shows the variations of the torque C as a function of the rotational speed of the rotor, keeping Ω_{id} constant. These trials have been done on the well known Shinsei USR60 [8].

In fact, in the neighbourhood of small torque, a linear approximation of the speed-torque curves is achievable, and the coefficient f of equation (18) can then be identified in that way.

On the other hand, an elastic layer is placed between stator and rotor, leading to an elastic potential energy accumulation on the normal axis:

$$F_N = K \int (V_{Nid} - V_N)\,\mathrm{d}t. \tag{19}$$

2.6 Effects of the contact mechanism

The relations obtained in the previous section allow to write the causal modeling of the TWUM. In references [4] and [9], the causal ordering graph (COG) tool has been used to represent the electromechanical coupling between voltage supply and traveling wave, and then the mechanical coupling between stator and rotor.

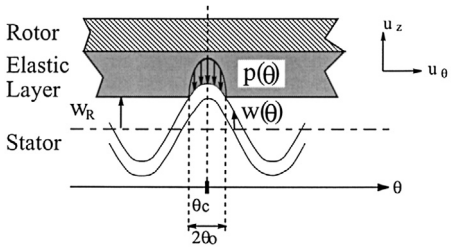

Fig. 5. Stator penetration in an elastic layer.

Even thought this modeling gave satisfactory results, it can be improved taking into account the effect of the contact length which settles at the stator-rotor interface.

When the contact between stator and rotor is punctual, the part of the modal forces due to the normal force F_N is simply expressed using the rotation matrix $R(k\theta_c)$:

$$\begin{pmatrix} f_{rn\alpha} \\ f_{rn\beta} \end{pmatrix} = R(k\theta_c) \begin{pmatrix} F_N \\ 0 \end{pmatrix}. \tag{20}$$

Nevertheless, an elastic layer is usually placed between the stator and the rotor in order to improve the motor's performance. The contact cannot be considered as punctual anymore, because the rigid stator comes into the contact layer (Fig. 5).

This has an influence on the calculation of $f_{rn\alpha}$ and $f_{rn\beta}$: equation (15) must be revised to take this phenomenon into account, which is what this section deals with.

The position in the z-direction of the rotor is called W_R, and the vertical displacement of the travelling wave, still supposed to be sinusoidal, is $w(\theta)$. The angular contact length is $2\theta_0$. Let $\theta' = \theta - \theta_c$, leading to:

$$w(\theta') = \hat{W} \cos(k\theta'). \tag{21}$$

2.6.1 Contact length

When forcing the stator in the z-direction with normal force F_N, a contact angular force distribution named $p(\theta')$ appears along the contact region (Fig. 5), so that we have:

$$F_N = k \int_{-\theta_0}^{\theta_0} p(\theta')\mathrm{d}\theta'. \tag{22}$$

The layer is modeled as a linear spring with equivalent angular stiffness C_N.

By definition of parameter C_N, the relationship between $p(\theta')$ and the stator penetration is

$p(\theta') = C_N\,(w(\theta') - W_R)$, leading to:

$$F_N = 2C_N \left(\hat{W} \sin(k\theta_0) - k\theta_0 W_R \right). \tag{23}$$

And the rotor position can be expressed using the contact length by: $w(k\theta_0) = W_R$:

$$W_R = \hat{W}\cos(k\theta_0). \tag{24}$$

Finally, the angle θ_0 is solution of the following equations (23, 24)

$$F_N = 2C_N\hat{W}(\sin(k\theta_0) - k\theta_0\cos(k\theta_0)). \tag{25}$$

We may remark that we cannot find out a solution to equation (24) for two cases. If $W_R > \hat{W}$, there is no contact zone; the modal forces are then null. If $W_R < -\hat{W}$, the contact layer is stuffing the rotor; the contact length is then $2k\theta_0 = 2\pi$.

2.6.2 Modal forces

The principle of the calculation of the modal forces is given by [2]:

$$\begin{pmatrix} f_{rn\alpha} \\ f_{rn\beta} \end{pmatrix} = k\int_{-\theta_0}^{\theta_0} \begin{pmatrix} \cos(k\theta) \\ \sin(k\theta) \end{pmatrix} p(\theta')\mathrm{d}\theta.$$

Integration is carried out over the contact's length, and equation (20) must be updated and replaced by:

$$\begin{aligned} \begin{pmatrix} f_{rn\alpha} \\ f_{rn\beta} \end{pmatrix} &= C_N W \begin{pmatrix} \cos(k\theta_c) \\ \sin(k\theta_c) \end{pmatrix} \left(k\theta_0 - \frac{\sin(2k\theta_0)}{2} \right) \\ &= R(k\theta_c) \begin{pmatrix} C_N\hat{W}\left(k\theta_0 - \frac{\sin(2k\theta_0)}{2}\right) \\ 0 \end{pmatrix}. \end{aligned} \tag{26}$$

It is important to notice that the rotational matrix can still be used. So, regarding the calculation of the part of the modal forces due to the normal force, and comparing equations (20, 26) the stator penetration may be considered substituting F_N by εF_N, with

$$\varepsilon = \frac{C_N\hat{W}\left(k\theta_0 - \frac{\sin(2k\theta_0)}{2}\right)}{F_N} \tag{27}$$

and

$$\begin{pmatrix} f_{rn\alpha} \\ f_{rn\beta} \end{pmatrix} = R(k\theta_c) \begin{pmatrix} \varepsilon F_N \\ 0 \end{pmatrix}. \tag{28}$$

2.6.3 Calculation of ε

Using (25) in (27) yields to the following equation:

$$\varepsilon = \frac{1}{2}\frac{k\theta_0 - \frac{\sin(2k\theta_0)}{2}}{\sin(k\theta_0) - k\theta_0\cos(k\theta_0)}. \tag{29}$$

Figure 6 shows the variation in ε along with the wave's amplitude $\hat{W}$ for a motor which key parameters are depicted Table 1.

Table 1. Parameters of a TWUM.

C_N	F_N	k	c
100 N/mm	300 N	11	5.55×10^9 N/m
m	d_s	AC_c	
75.5 g	238 Nsm^{-1}	0.32 N/V	

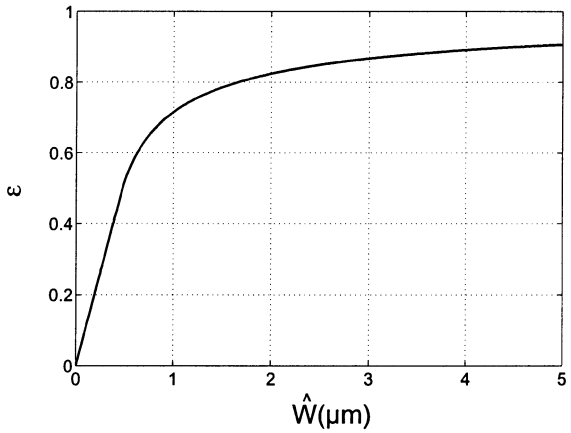

Fig. 6. Variations in ε.

On this curve, we can observe that for the high wave amplitudes, $\varepsilon = 1$ which means the contact condition comes close to punctual. On the opposite, when the stator is stuffed by the rotor, $\varepsilon = 0$ and the normal force has no effect on the wave.

Some authors replace εF_N by a stiffness variation [10]; the parameter c of equation (10) is changed in $c + \tilde{c}$, with $\tilde{c} = \frac{\varepsilon F_N}{\hat{W}}$. The stiffness is then a function of the wave's amplitude, and this is how the *pull out* phenomenon is explained, and therefore taken into account in the modeling.

2.6.4 Normal speed of the ideal rotor

The virtual work theorem used in Section 2.4 must still work, even though the contact is not punctual, and we write again:

$$\begin{aligned} \delta p &= -f_{r\alpha}\delta\dot{w}_\alpha - f_{r\beta}\delta\dot{w}_\beta \\ &= -(\varepsilon F_N\cos(k\theta_c) - F_T'\sin(k\theta_c))\delta\dot{w}_\alpha \\ &\quad - (\varepsilon F_N\sin(k\theta_c) + F_T'\cos(k\theta_c))\delta\dot{w}_\beta \\ &= -F_N\varepsilon(\cos(k\theta_c)\delta\dot{w}_\alpha + \sin(k\theta_c)\delta\dot{w}_\beta) \\ &\quad - F_T'(\cos(k\theta_c)\delta\dot{w}_\beta - \sin(k\theta_c)\delta\dot{w}_\alpha) \\ &= F_T\delta V_{Tid} - F_N\varepsilon\delta V_{Nid}. \end{aligned} \tag{30}$$

Then it appears that the expression for the normal speed must be modified in:

$$V_{Nid} = \varepsilon(\dot{w}_\alpha\cos(k\theta_c) + \dot{w}_\beta\sin(k\theta_c)). \tag{31}$$

2.6.5 Modeling comparison

This study leads to a causal modeling which can be depicted by a COG with the same structure as in [9], but

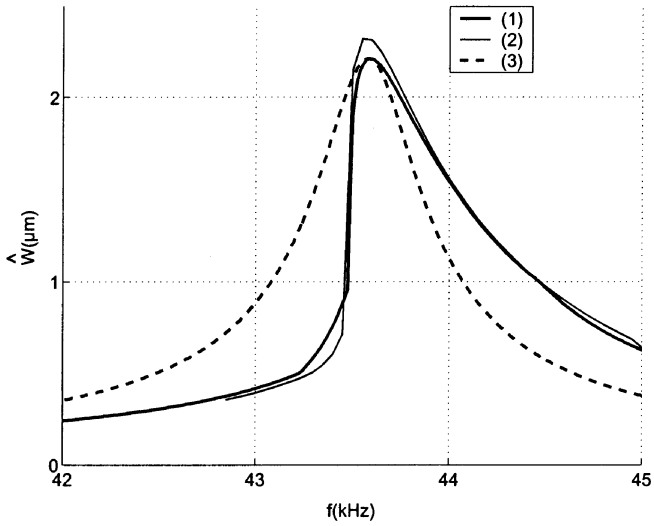

Fig. 7. Comparison of several modelings 1: Causal modeling 2: Modeling approaching the contact mechanism by the Coulomb's law (reference modeling) 3: EEC modeling.

which takes the contact repartition into account through the parameter ε.

On one hand, this modelization is first compared with a reference modeling which approaches the contact mechanism by the Coulomb's friction law. We have drawn in Figure 7 the traveling wave's amplitude of the stator's vibration as a function of the frequency of two sinusoidal voltages with constant RMS value feeding the actuator. The results are computed for the motor with parameters depicted Table 1; no torque is applied on the shaft, and the motor have reached the steady-state. Both modeling fit together: the position of the crest is located at the same place, and the well known pull-out phenomenon, responsible for the asymmetrical characteristic, appears even though the causal modeling means a globalization of the contact mechanism.

On the other hand, because an electrical equivalent circuit (EEC) is often used to describe piezo actuators, we have also drawn on the same figure its response for the same operating conditions. The parameters used are deduced from m, c and d_s, thanks to [3]. This modeling does not take into account the effect of the normal pressure on the wave, and this is the main difference from the causal modeling.

But according to Figure 7 the response of the EEC does not fit the reference modeling: the pull out phenomenon cannot be taken into account, and the crest is thinner. Even though it is possible to refine the value of the parameters, so as to fit the modelings together [11] for frequencies above the resonance, these last parameters identified from straightforward experimental trials are then different from those available from the proposed causal modeling.

This analyse, achieved on a TWUM whose interface parameters are depicted Table 1, shows then that an other identification method is needed for the proposed causal modelling. This method is detailed further; it is based on a modelling in a rotating reference frame which is first described.

3 Modelization in the traveling wave's rotating frame

The two rotational matrices appearing in (15) and (9) reminds us of the classical electromagnetic machines for which a modeling in a rotating frame is often used to serve a control scheme.

The aim of this section is to apply the same reasoning to Traveling Wave Ultrasonic Motors; actions along normal and tangential axis will be decoupled, which is helpful to achieve a control scheme as it is already described in [4]. But it can also be used for the parameters identification of the TWUM which is now developed.

So, we are brought to set down:

$$\begin{pmatrix} v_\alpha \\ v_\beta \end{pmatrix} = R(k\theta_c) \begin{pmatrix} v_d \\ v_q \end{pmatrix} \tag{32}$$

and

$$\begin{pmatrix} i_{m\alpha} \\ i_{m\beta} \end{pmatrix} = R(k\theta_c) \begin{pmatrix} i_{md} \\ i_{mq} \end{pmatrix}. \tag{33}$$

Because equation (9) can also be written as:

$$\begin{pmatrix} \dot{w}_\alpha \\ \dot{w}_\beta \end{pmatrix} = R(k\theta_c) \begin{pmatrix} V_{Nid} \\ V'_{Tid} \end{pmatrix}$$

we can write:

$$\begin{aligned} \begin{pmatrix} \ddot{w}_\alpha \\ \ddot{w}_\beta \end{pmatrix} &= \frac{\mathrm{d}}{\mathrm{d}t} \left(R(k\theta_c) \begin{pmatrix} V_{Nid} \\ V'_{Tid} \end{pmatrix} \right) \\ &= R(k\theta_c) \begin{pmatrix} \dot{V}_{Nid} \\ \dot{V}'_{Tid} \end{pmatrix} \\ &\quad + k\dot{\theta}_c R\left(k\theta_c + \frac{\pi}{2}\right) \cdot \begin{pmatrix} V_{Nid} \\ V'_{Tid} \end{pmatrix}. \end{aligned} \tag{34}$$

Moreover, using equations (9) and (4), it is possible to find out an other expression for the stationary wave's vector:

$$\begin{aligned} \int V_{Nid}\mathrm{d}t &= \int \left(\dot{w}_\alpha(t)\cos(k\theta_c) + \dot{w}_\beta(t)\sin(k\theta_c)\right)\mathrm{d}t \\ &= \left[w_\alpha \cos(k\theta_c) + w_\beta \sin(k\theta_c)\right] \\ &\quad \underbrace{- \int k\dot{\theta}_c \left(-w_\alpha \sin(k\theta_c) + w_\beta \cos(k\theta_c)\right)\mathrm{d}t}_{0} \end{aligned}$$

yielding to the following equation:

$$\begin{pmatrix} \int V_{Nid}\mathrm{d}t \\ 0 \end{pmatrix} = R(-k\theta_c) \begin{pmatrix} w_\alpha \\ w_\beta \end{pmatrix}$$

or

$$\begin{pmatrix} w_\alpha \\ w_\beta \end{pmatrix} = R(k\theta_c) \begin{pmatrix} \int V_{Nid}\mathrm{d}t \\ 0 \end{pmatrix}. \tag{35}$$

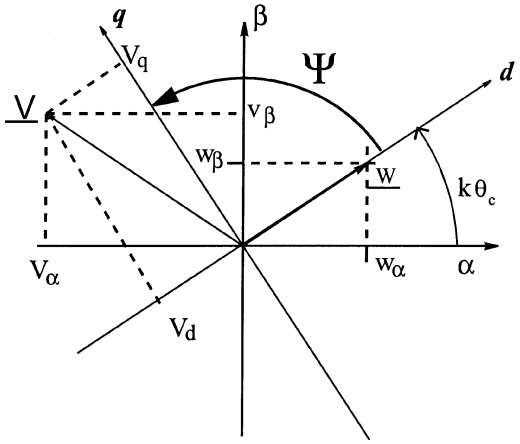

Fig. 8. Definition of the wave's reference frame and the associated space vectors $\underline{v} = v_\alpha + jv_\beta$, $\underline{w} = w_\alpha + jw_\beta$.

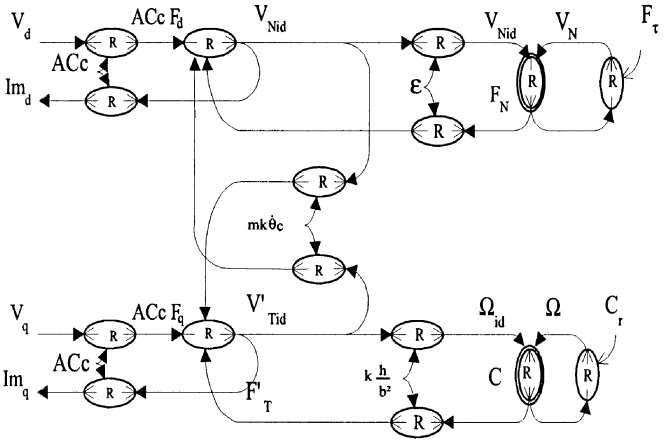

Fig. 9. Causal Ordering Graph in the rotating frame.

This expression may be illustrated by Figure 8, where we can see the new rotating axis d located on the wave space vector.

Under consideration of this variables change, it is possible to rewrite equation (10) which describes the stator's vibration:

$$mR(k\theta_c)\left[\begin{pmatrix}\dot{V}_{Nid}\\ \dot{V}'_{Tid}\end{pmatrix} + k\dot{\theta}_c R(\frac{\pi}{2})\begin{pmatrix}V_{Nid}\\ V'_{Tid}\end{pmatrix}\right] + d_s R(k\theta_c)\begin{pmatrix}V_{Nid}\\ V'_{Tid}\end{pmatrix} + cR(k\theta_c)\begin{pmatrix}\int V_{Nid}\mathrm{d}t\\ 0\end{pmatrix} = AC_cR(k\theta_c)\begin{pmatrix}V_d\\ V_q\end{pmatrix} - R(k\theta_c)\begin{pmatrix}\varepsilon F_N\\ F'_T\end{pmatrix}.$$

And thanks to the rotational matrix properties, we find the equations governing the evolution of the normal and tangential speed of the ideal rotor.

$$m\dot{V}_{Nid} + \mathrm{d}_s V_{Nid} + c\int V_{Nid}\mathrm{d}t = AC_cV_d - \varepsilon F_N + mk\dot{\theta}_c V'_{Tid} \quad (36)$$

$$m\dot{V}'_{Tid} + d_s V'_{Tid} = AC_cV_q - F'_T - mk\dot{\theta}_c V_{Nid}. \quad (37)$$

These equations are outstandingly important because they help to dissociate the dynamic of both the degrees of freedom of the TWUM. Equation (36), because it makes V_{Nid} and F_N appear, is the equation for the normal axis, and equation (37) is for the tangential axis.

The COG of Figure 9 highlights the d and q axis of the TWUM as well as the coupling terms. The COG building is explained in [12] and [13].

The TWUM have many non linearities, such as the variation in c with the temperature, or ε with the wave's amplitude. But these non-linearities, concentrated into one equation, do not appear anymore in the torque equation. Moreover, equation (37) is a 1st order equation. It has been shown in [7] how this frame change helped to linearize the dynamic of the stator. The next section capitalizes on these advantages, in order to achieve an identification of the stator's parameters.

4 Identification of the stator's parameters of the TWUM

4.1 Principle

The aim of this method is to achieve an identification of the stator parameters m, c and d_s.

The process is based on two tries: steady state try and transitory try. All along these three following sections, the motor is free, and the inertia effects are neglected.

Steady state measurements

For steady state operation, because $F'_T = 0$ and $V_{Nid} = 0$, equation (37), lets us write:

$$d_s V'_{Tid} = AC_cV_q. \quad (38)$$

So, the relationship between V'_{Tid} and V_q, which must be linear, gives us the coefficient d_s. During the experiment, $V_d^2 + V_q^2 = V^2$ so as to control the line voltages V_α and V_β.

Transitory operation

When V_q is step varying, the transient response of the ideal rotor tangential speed is expressed from equation (37):

$$m\dot{V}'_{Tid} + dsV'_{Tid} = AC_cV_q - mk\dot{\theta}_c V_{Nid}. \quad (39)$$

The cross coupling term $mk\dot{\theta}_c V_{Nid}$ is troubling; but it is possible to find a less troubling expression for it. In fact,

we have:

$$\begin{aligned}\begin{pmatrix}\dot{w}_\alpha\\ \dot{w}_\beta\end{pmatrix} &= \frac{\mathrm{d}}{\mathrm{d}t}\left[R(k\theta_c)\begin{pmatrix}\int V_{Nid}\mathrm{d}t\\ 0\end{pmatrix}\right]\\ &= R(k\theta_c)\begin{pmatrix}V_{Nid}\\ 0\end{pmatrix}\\ &\quad + k\dot{\theta}_c R(k\theta_c+\frac{\pi}{2})\begin{pmatrix}\int V_{Nid}\mathrm{d}t\\ 0\end{pmatrix}\\ &= R(k\theta_c)\begin{pmatrix}V_{Nid}\\ k\dot{\theta}_c\int V_{Nid}\mathrm{d}t\end{pmatrix}.\end{aligned}$$

Comparing this result to the one of equation (9), we can write a new expression for V'_{Tid}: $V'_{Tid} = k\dot{\theta}_c \int V_{Nid}\mathrm{d}t$, leading to: $\dot{V}'_{Tid} = k\dot{\theta}_c V_{Nid} + k\ddot{\theta}_c \int V_{Nid}\mathrm{d}t$. So, the cross coupling term $k\dot{\theta}_c V_{Nid}$ can be fortunately expressed as follows: $k\dot{\theta}_c V_{Nid} = \dot{V}'_{Tid} - k\ddot{\theta}_c \int V_{Nid}\mathrm{d}t$. In very resonant structure, $k\ddot{\theta}_c \int V_{Nid}\mathrm{d}t$ is not significant. So, equation (39) can be approximated by:

$$2m\,\dot{V}'_{Tid} + d_s\,V'_{Tid} = AC_c\,V_q.$$

The response of V'_{Tid} to a V_q step change is a 1st order type, the time constant of which is $\tau = \frac{2m}{d_s}$. Measuring this constant helps to find parameter m; c is deduced from the value of the resonance frequency of the motor f_o:

$$c = (2\pi f_o)^2 m. \tag{40}$$

4.2 Experimental scheme

The drawing of the complex phasors higligths the angle between $\underline{V}$ and $\underline{W}$, called Ψ. And the projection of the voltage phasor on the axis d and q let us write $V_d = V\cos(\Psi)$, and $V_q = V\sin(\Psi)$. We make the assumption that there is no cross coupling between the two stationary waves, so as to we can write:

$$w_\alpha(t) = \hat{W}\cos(\omega t) \qquad w_\beta(t) = \hat{W}\sin(\omega t) \tag{41}$$

leading to $k\theta_c = \omega t$ and $V'_{Tid} = \omega\hat{W}$ (ω is the line voltage frequency). As the tangential speed V'_{Tid} cannot be directly measured, it is replaced in (38) and the mechanical transfer function $\frac{\hat{W}}{V}$ can be expressed as a function of Ψ:

$$\frac{\hat{W}}{V} = \frac{AC_c}{d_s\omega}\sin(\Psi). \tag{42}$$

For $\Psi = 90°$, equation (42) directly gives $\frac{AC_c}{d_s\omega}$.

Moreover, it has been proven that a non linearity about the wave's amplitude can appear in the mechanical resonator [14]. This is why the experiments will be realized keeping constant this amplitude. Considering that an auxiliary electrode measures the position of $\underline{W}$ a dephasor, realized with a Phase Locking Loop, imposes the angle Ψ. Linear amplifiers feed then the motor. This experimental scheme is detailed in [7] and [15].

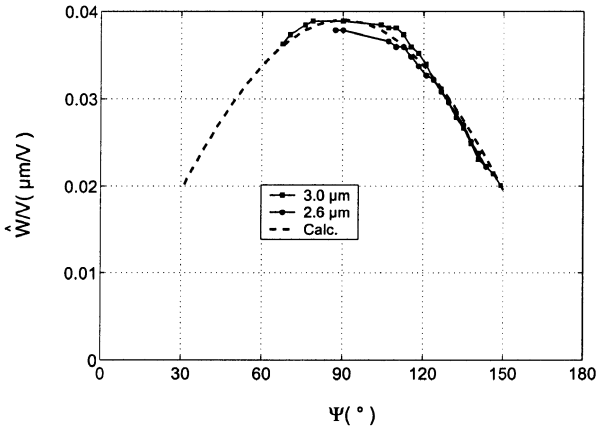

Fig. 10. Transfer function at constant wave amplitude.

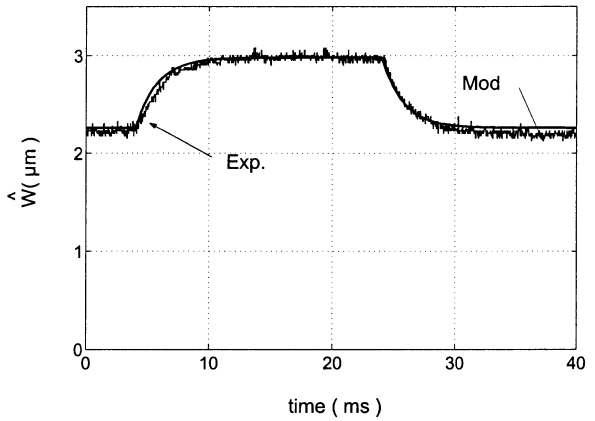

Fig. 11. Wave amplitude response to V_q steps.

4.3 Experimental results

This identification method has been tested on the well known Shinsei USR60; its parameters are different from those of the motor depicted Table 1.

Steady state measurement

We have drawn in Figure 10 the mechanical transfer function for two wave's amplitude, and the model prediction.

The model quite fits with the experiments and the shapes are quite the same. Using these results and with the help of equation (42), a value for d_s can be deduced, and we finally have $d_s = 32Ns/m$.

Transitory operation

According to Section 4.1, we can find the parameter m measuring the time constant of a V_q step response of the travelling wave's amplitude. Figure 11 depicts such a response.

Finally, we find $m = 28 \times 10^{-3}$ kg. The stator's resonance frequency is about 40.2 kHz, leading to $c = 1.78\,\mathrm{e}9$ N/m.

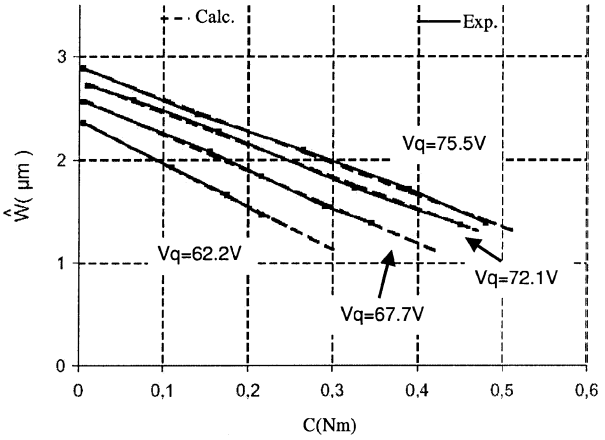

Fig. 12. Travelling wave's amplitude as a function of the torque, V_q maintained constant.

4.4 Experimental validation with a loaded motor

For steady state operation, and making assumption (41), equation (37) becomes:

$$d_s\omega\hat{W} = AC_cV_q - F'_T. \tag{43}$$

From the definitions of F_T and F'_T, equation (43) leads to:

$$d_s\omega\hat{W} = AC_cV_q - k\frac{h}{b^2}C. \tag{44}$$

Thus, the variation in the stationary wave's amplitude $\hat{W}$ with V_q constant as a function of the torque C must be linear. This is validated by the experimental try of Figure 12.

Moreover, the parameter h, which can be deduced from that try and (44), is in a good accordance with the value deduced from a mechanical study [5].

5 Conclusion

In this article, we have shown a modelization of a travelling wave type ultrasonic motor. The ideal rotor assumption helped to simplify the equations, and the use of the already well known rotational matrice is highlighted. We have compared this modeling with the electrical equivalent circuit; we have shown that the values of the stator's parameters identified by a equivalent circuit are not the same as those for the causal modeling.

Identification of the parameters of the motor is then closely studied; a modeling in the wave's rotating frame is established and a new identification method is explored. The main advantage of this method is to not need the contact conditions to determine the desired parameters.

This approach can be successfully extended to other travelling wave type motors [16]. As a perspective to this work, we could try to know if the values found with this method are consistent to those calculated by a finite element method.

References

1. Canon, Vibration driven motor Patent CA2048400
2. J. Maas, P. Ide, N. Fröhleke, H. Grostollen, Simulation model for ultrasonic motors powered by resonant converters, *IAS'95*, Vol. 1, pp. 111–120, October (1995)
3. T. Sashida, T. Kenjo, *An introduction to Ultrasonic Motors* (Clarendon Press, 1993)
4. F. Giraud, B. Lemaire-Semail, J.-P. Hautier, Model and control of a travelling wave ultrasonic motor, *EPE 2001*, August 2001
5. C. Giraud-Audine, *Contribution à la modélisation analytique d'actionneurs piézo-électriques en vue de leur conception et dimensionnement*, Ph.D. thesis, INP Toulouse, 1998, N1501
6. W. Hagood IV, A.J. McFarland, IEEE Trans. Ultrason. Ferroelectr. Frequency Control **42**, 210 (1995)
7. F. Giraud, B. Lemaire-semail, Commande en phase d'un moteur piézo-électrique à onde progressive, *Magelec*, pp. 189–193, December 2001
8. Website, `http://www.tky.3web.ne.jp/usrmotor/`
9. F. Giraud, B. Semail-Lemaire, J.-P. Hautier, Modèle dynamique d'un moteur piezo-électrique à onde progressive, *RIGE*, Vol. 4, pp. 411–430, avril 2001
10. J. Maas, H. Grostollen, IEEE Power Electron. Specialists Conf. (PESC) **1**, 740 (1997)
11. N. El ghouty, *Hybrid modeling of a traveling wave piezo electric motor*, Ph.D. thesis, Aalborg University, department of control engineering, May 2000
12. J.P. Hautier, J.P. Caron, *Les convertisseurs statiques : méthodologie causale de modélisation et de commande*, Editions Technip, 1998
13. X. Guillaud, P. Degobert, J.-P. Hautier, P.-J. Barre, Synthesis of control laws with the causal ordering graph: Application to elimination of vibration in drive of mechanical laws, *ICEM 2000*, pp. 1917–1921
14. A. Albareda, P. Gonnard, V. Perrin, R. Briot, D. Guyomar, IEEE Trans. Ultrason. Ferroelectr. Frequency Controls **47**, 844 (2000)
15. F. Giraud, *Modélisation causale et commande d'un actionneur piézo-électrique à onde progressive*, Ph.D. thesis, Université Lille I, 2002
16. M. Budinger, F. Giraud, B. Nogarède, J.-F. Rouchon, B. Lemaire-Semail, Feeding and control electronic of a piezoelectric actuator, *ACTUATOR 2002*, to be published